SUPPLEMENT TO THE *WELDING JOURNAL*, NOVEMBER 2003
Sponsored by the American Welding Society and the Welding Research Council

Effects of Electrode Degradation on Electrode Life in Resistance Spot Welding of Aluminum Alloy 5182

Degradation of electrode tip faces increased the contact area at the electrode/sheet interface, which resulted in an undersized nugget at the sheet/sheet interface

BY S. FUKUMOTO, I. LUM, E. BIRO, D. R. BOOMER, AND Y. ZHOU

ABSTRACT. Electrode endurance tests were conducted to investigate the effects of electrode degradation on electrode life in resistance spot welding of 1.5-mm-thick sheet aluminum Alloy 5182 using a medium-frequency direct-current welding machine and electrodes with tip-face diameter of 10 mm and radius of curvature of 50 mm. The observed electrode life ranged from about 400 to 900 welds even though all the process conditions were intentionally kept constant. However, despite the large variation, distinct patterns were found to correlate electrode life to electrode degradation in terms of the change in nominal electrode tip-face area and contact areas at both electrode/sheet (E/S) and sheet/sheet (S/S) interfaces. The reduction in joint strength occurred because of undersized nugget formation due to increased contact areas and hence reduced current density. The electrode degradation may be monitored by the increase in all three areas (nominal tip-face area, and E/S and S/S contact areas), but the E/S contact area is believed to be the most suitable because a minimum of extra work is needed to measure it. The button diameter, measured from peel testing, is affected by nugget diameter (current density) and possibly other factors, such as weld expulsion and porosity distribution as well.

Introduction

The interest in high-volume production of aluminum parts for vehicle applications has been growing rapidly in the last decade because of the growing pressure from legislation to improve fuel efficiency and reduce vehicle emissions (Ref. 1). Resistance spot welding (RSW) is one of the most attractive assembly methods because it is simple in operation and low in cost. Therefore, there is an increased emphasis on high-volume RSW of aluminum to support its use in production. .

Resistance spot welding of aluminum continues to suffer from two major problems: inconsistent weld quality and short electrode life (Ref. 2). Electrode life in RSW of aluminum varies considerably depending on testing conditions, such as electrode design, which includes copper alloy selection (Refs. 3, 4), coating (Ref. 5), and configuration (Refs. 4, 6); and sheet (Refs. 7, 8) and electrode (Ref. 9) surface conditions. For example, it has been reported that electrode life ranged from 950 to 1700 welds with truncated cone electrodes and from 300 to 450 welds with domed electrodes (Ref. 4). However, detailed research work on electrode degradation and its correlation to electrode life during RSW of aluminum has been quite limited (Ref. 10).

A previous study (Ref. 11) on electrode degradation has been performed on RSW of 1.5-mm-thick sheet aluminum alloy 5182 using a medium-frequency direct-current (MFDC) welding machine and electrodes with tip-face diameter of 10 mm and radius of curvature of 50 mm. The metallurgical interactions between the copper electrode and aluminum sheet were analyzed using scanning electron microscopy/energy-dispersive X-ray spectroscopy and X-ray diffraction. The results indicated that electrode degradation, which eventually leads to electrode failure, could form in four steps: aluminum pickup, electrode alloying with aluminum, electrode tip-face pitting, and cavitation. Since pitting and cavitation are results of Al pickup and alloying, periodic electrode cleaning could extend electrode tip life by limiting the buildup of Al on the tip faces. The present work will focus on the effects of electrode degradation on electrode tip life in RSW of aluminum Alloy 5182.

KEYWORDS

Aluminum Alloy 5182
Resistance Spot Welding
Electrode Degradation
Electrode Tip Life

Experimental Procedure

Welds were made on 1.5-mm-thick, electrolytically cleaned aluminum alloy sheet AA5182-H111 (Table 1), supplied by Alcan International Ltd., using a 170-kVA MFDC pedestal resistance spot welding machine. No cleaning was performed on the sheet surface prior to welding. All tests used Class 1 (Cu-0.15% Zr) electrodes with taper angle of 60 deg, and tip-face diameter of 10 mm and radius of curvature of 50 mm — Fig. 1. Before being installed on the welding machine, the electrode tip faces were cleaned with a Scotchbrite® abrasive pad until all visible surface oxide was removed.

The welding conditions for the electrode life tests (Table 2) were determined through weld lobe tests (Ref. 10). Carbon imprinting was done by sinking the electrode tips into carbon and plain white papers placed onto an aluminum sheet using the electrode force and duration shown in Table 2. Electrode life tests were performed on coupons of 50 × 400 mm (10 welds per coupon set) with 35 mm spacing

S. FUKUMOTO is with Department of Materials Science and Engineering, Faculty of Engineering, Himeji Institute of Technology, Himeji, Hyogo, Japan. I. LUM, E. BIRO, and Y. ZHOU are with Department of Mechanical Engineering, University of Waterloo, Waterloo, Ontario, Canada. D. R. BOOMER is with Banbury Laboratory, Alcan International Limited, Banbury, Oxfordshire, U.K.

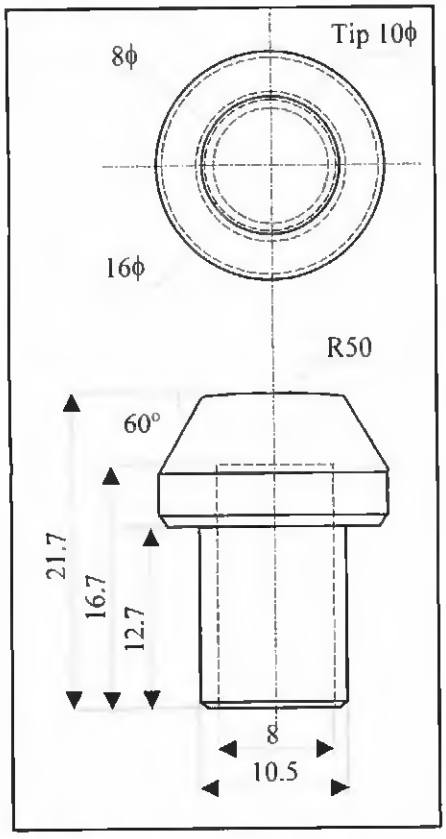

Fig. 1 — Configuration of the electrode (unit: mm).

between welds. Shear tests (of five samples) were performed every 50 welds before 500 welds, and subsequently every 100 welds on single-weld coupons of 30 × 120 mm — Fig. 2. In shear testing, restraining shims were used to minimize the rotation of the joints and maintain the shear loading for as long as possible (Ref. 12). Testing was performed using an Instron (Model 4206) tensile testing machine with a load cell of 15,000 kg and a cross-head speed of 0.33 mm/s. The maximum shear force was recorded and used as an indication of joint strength. Electrode tip life was defined as the first weld number when the joint strength dropped below 80% of its initial value.

Nominal and actual tip-face areas were defined, respectively, as the area based on the outside diameter of the carbon imprint, and the nominal area less the pitted area, also measured from carbon imprints. The contact area at the electrode/sheet (E/S) interface was measured after welding based on the outside diameter of the electrode imprint on the sheet surface. It should be kept in mind that the nominal tip-face area would be smaller than the E/S contact area since the electrode tip would sink more into the aluminum sheet during welding because the yield strength of the sheet is lowered at high temperature and the welding force remains constant. The contact area at the sheet/sheet (S/S) interface and nugget area was measured from fractured faying surfaces after shear testing, in which the S/S contact area was based on the outside diameter of the indentation produced by the S/S interactions during welding. All the area measurements were done using a computer-based image analyzer.

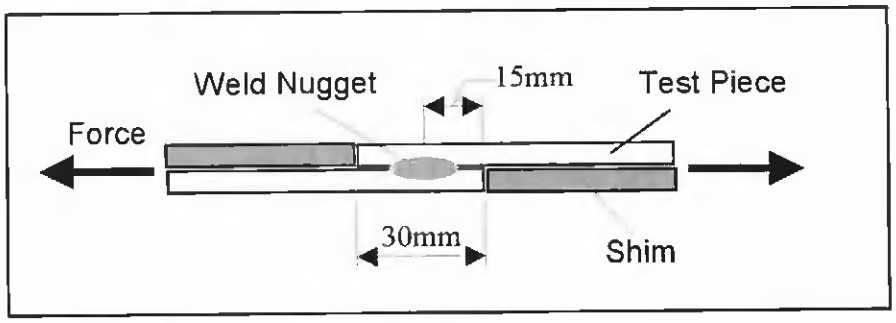

Fig. 2 — The setup for tensile shear testing.

Table 1 — Chemical Composition of AA 5182

Element	Si	Fe	Cu	Mn	Mg	Al
Mass-%	0.08	0.19	0.05	0.32	4.71	Bal.

Table 2 — Welding Parameters

Squeeze	25 cycles
Weld Time	5 cycles
Hold Time	12 cycles
Weld Force	6 kN
Welding Current	29 kA
Welding Rate	20/min

Results

Electrode Life Test

The maximum shear forces (as an indication of joint strength) were plotted as a function of weld numbers (Fig. 3), in which each data point shows the average of five shear test samples and the range with plus/minus one standard deviation. These were the typical data sets selected from six electrode life tests. All those tests indicated a tip life ranging from 400 to 900 welds in nominally identical electrode life tests (data sets) even though all the process conditions were intentionally kept constant. Despite the large variation in electrode life, distinct patterns were found to exist.

- Stage 1: At the beginning of electrode tip life, the shear force, starting at 500–550 kg, was relatively constant (e.g., up to 240 welds in data set 2).
- Stage 2: In this period, the shear force increased with increasing weld number and peaked at 600–650 kg. It is believed that the increase in shear force was due to the alloying and incipient pitting on the electrode tip face (Ref. 11).
- Stage 3: After reaching the maximum, the shear force started to decrease until dropping below 80% of the initial value, indicating the end of tip life.

Almost all the joints fractured as interfacial failures, with only a few with larger nugget diameter failing as button pullouts because of the rotation of the sample joint during testing (Refs. 10, 12). Fractured surfaces of shear-tested joints are shown in Fig. 4, in which hand-drawn circles surrounding the fractured nuggets indicate the maximum contact area at the S/S interface during welding. At the beginning of the tip life test, the nugget was round, with an area about 37 mm^2 located at the center of the contact area. The nugget area increased slightly with increasing weld number and peaked at around 180, 360, and 180 welds, respectively, for data sets 1, 2, and 3. The nugget was still round and centered at this stage. After the peak, the nugget started to decrease in size, changed to an oval shape, and drifted away from the center. Eventually, the nugget became very small and irregular in shape and wandered around. Electrode failure coincided with this stage.

When shear force was plotted against nugget area (Fig. 5), a simple linear relationship was found between the two, which indicates that, since shear force was determined by nugget area, undersized nugget was responsible for electrode failure — Fig. 3. The gradient of the linear relationship in Fig. 5 was approximately 140 MPa, which is really the joint material's shear strength. This value is reasonable considering that the shear strength of 5000 series aluminum alloys (O temper) ranges from 125 to 186 MPa (Ref. 13). One of the reasons for the scatter in Fig. 5 might be that true shear loading is hard to maintain in this type of strength test (Ref. 12).

Electrode Degradation

The carbon imprints of the electrode tip faces (Fig. 6), which provide an indica-

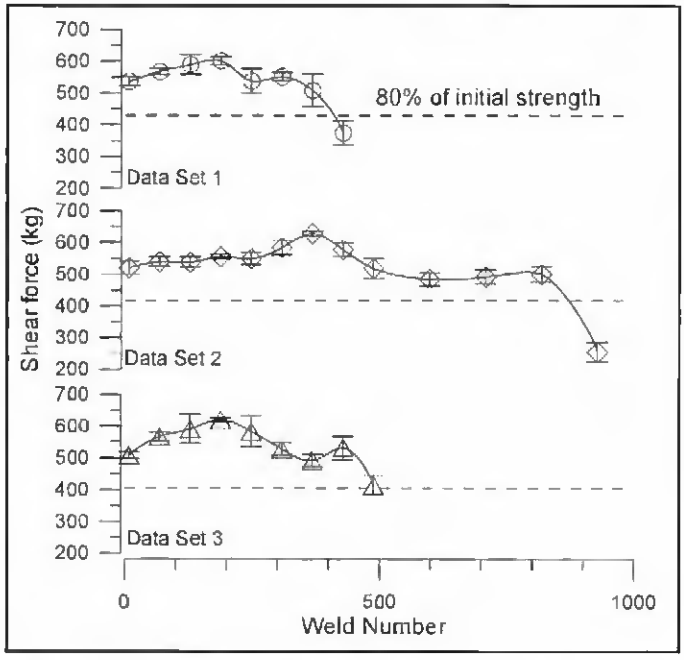

Fig. 3 — Shear failure load of welded joint vs. weld number.

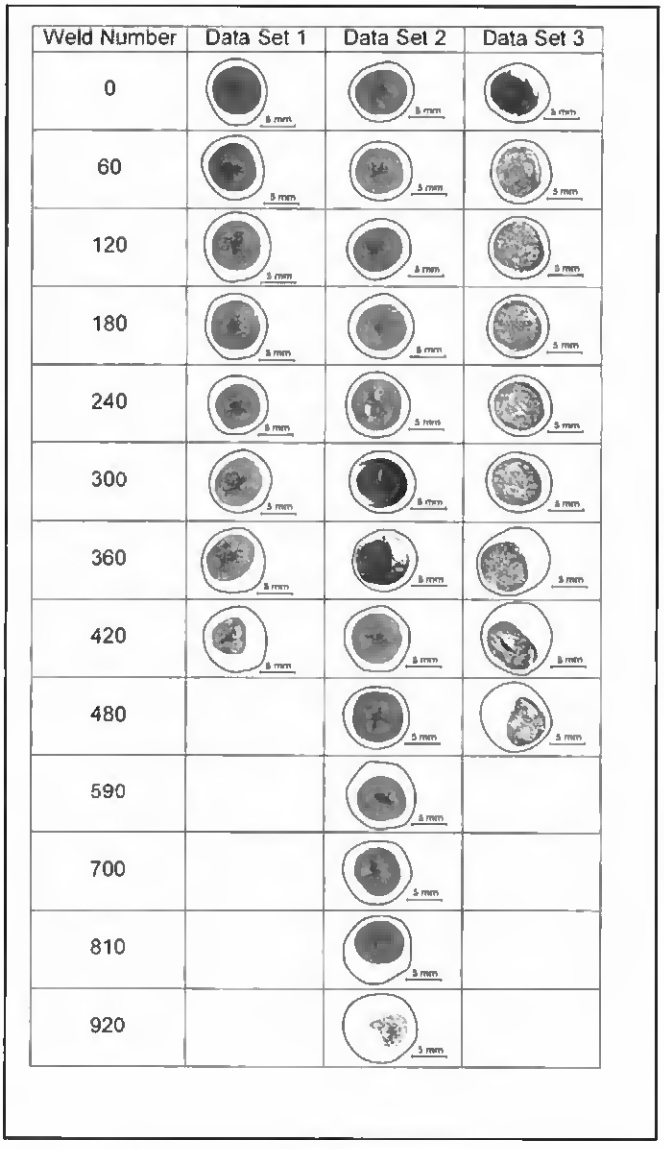

Fig. 4 — Fractured nuggets in electrode life test.

tion of the tip face morphology, could be used to monitor the progress of electrode degradation. It can be seen from Fig. 6 that electrode degradation was more significant on the top electrode than on the bottom electrode, which is consistent with the polarity effect since top and bottom electrodes remain positive and negative, respectively, during welding. According to the Peltier effect (Ref. 14), the heat generation will be higher at the top tip face than at the bottom tip face, which would speed up the electrode degradation at the top junction. The following discussion will concentrate on the behavior of the top electrodes.

Similar to the patterns observed on the joint strength, the morphology of the electrode tip face appeared to change in three stages.

- Stage 1: There was little change on the tip faces in terms of diameter and pitting (e.g., up to 60, 300, and 60 welds, respectively, for data sets 1, 2, and 3).
- Stage 2: Electrode pitting initiated at about 65, 340, and 90 welds, respectively, for sets 1, 2, and 3 at the edge regions of tip faces, judging from direct visual observation. Eventually, the pits grew and connected to each other, forming roughly a ring pattern (shown in Fig. 6 at 120, 360, and 120 welds, respectively, for data sets 1, 2, and 3). This was also the stage when the joint strength reached its maximum.
- Stage 3: The ring pits grew mainly inward and slightly outward, until the central portions of the tip face were consumed (completely pitted away) and the electrodes failed. After electrode failure, the contacting regions on the tip face became more asymmetrical and scattered.

Figure 7 shows both nominal and actual tip-face areas, along with the S/S and E/S contact areas. The nominal tip-face area remained relatively constant prior to electrode pitting (e.g., up to 300 welds in data set 2). It started to increase after the onset of electrode pitting (i.e., loss of material at the contact tip face [Ref. 11]), while the actual tip-face area remained fairly constant over the entire electrode life. This is reasonable because the pitted tip face (with an initial radiused profile) would sink into the sheet during carbon imprinting until the same level of actual contact area was reached to resist the same electrode force. Electrode life ended when the nominal tip-face area reached 60–70 mm^2.

Once pitting started, the nominal tip-face area (based on the carbon imprint) approached the E/S contact area although the E/S contact area was larger than the nominal tip-face area at the beginning due to the difference in temperature history as described in the experimental section — Fig. 7. This may be because, as the tip face became more pitted and flattened, some of the pitted regions would sink into the aluminum sheet to carry the electrode force during carbon imprinting and weld-

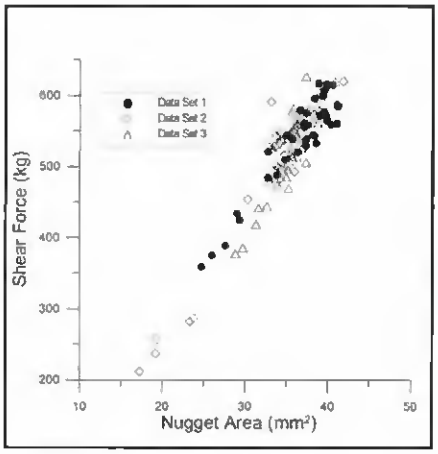

Fig. 5 — The relation between nugget area and shear force.

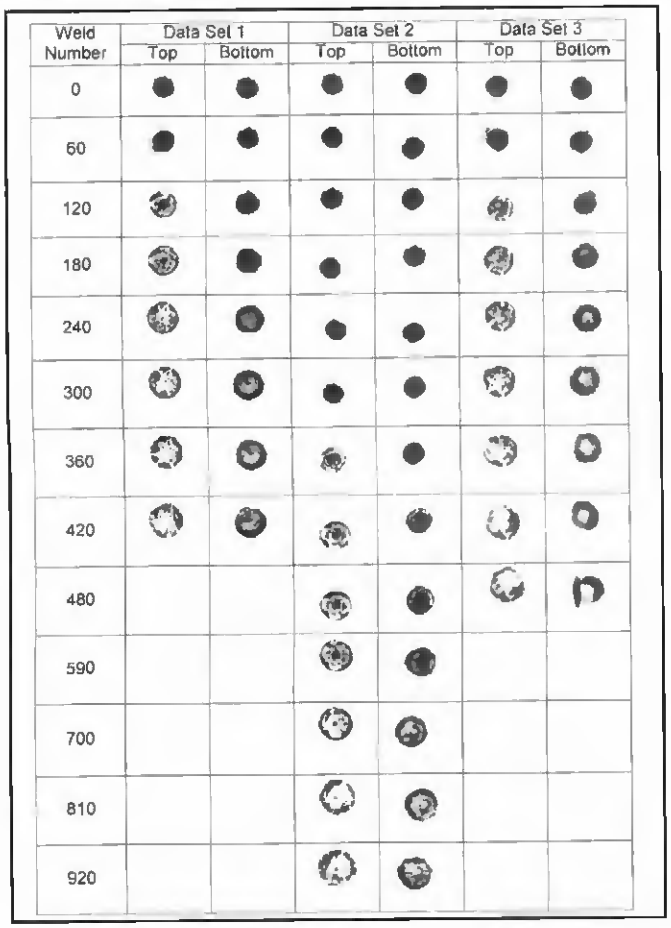

Fig. 6 — Carbon imprints of electrode tip face.

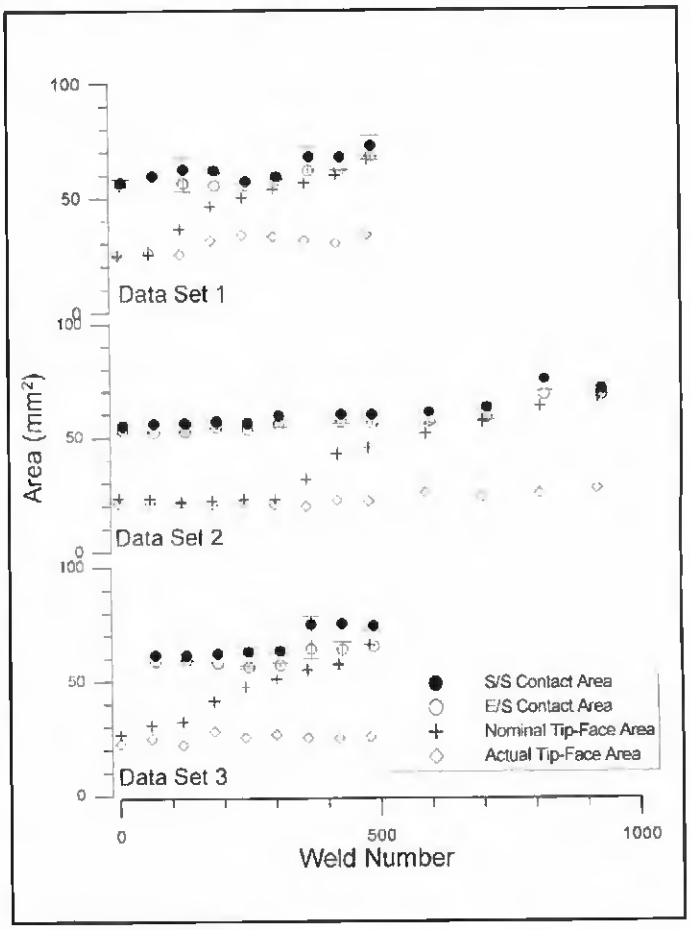

Fig. 7 — The variations of contact areas during electrode life tests.

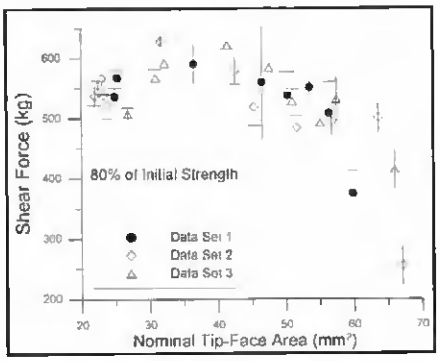

Fig. 8 — Relation between shear force and nominal tip-face area.

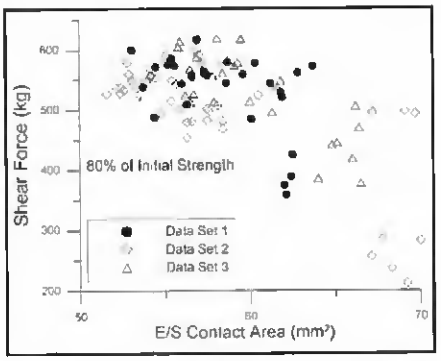

Fig. 9 — Relation between shear force and E/S contact area.

ing, which would reduce the difference between these two (nominal) areas. But, it is clear that the increase in nominal tip-face area resulted in an increase in the contact areas at both E/S and S/S interfaces.

Discussion

Electrode Life

As pointed out in the results section, the joint (and hence the electrodes) failed because of undersized nuggets, which appeared to correlate to the changes that occurred on the electrode tip faces. Those changes, in turn, resulted in an increase in the contact areas at both E/S and S/S interfaces, and hence the area of current distribution (i.e., reduced current density). Figures 8, 9, and 10 show the relations between joint strength and the nominal tip-face area, and the E/S and S/S contact areas, respectively.

The joint strength increased with increasing nominal tip-face area at first (Fig. 8), which is believed to be due to the alloying and initial pitting on the electrode tip face (Ref. 11). After reaching its maximum, the joint strength decreased with increasing tip-face area, which is believed to he due to the increase in contact areas at the E/S and S/S interfaces — Fig. 7. It can be seen that the joint strength generally dropped below 80% of its initial value when the tip-face area was larger than 60 mm^2.

Similar trends can be found in Figs. 9 and 10, in which the electrode failed when the contact areas at the E/S and S/S interface were at about 62 and 65 mm^2, respectively. It is interesting to note that there are roughly two data groups in both Figs. 9 and 10, with the first before electrode failure and second after the failure. The comparison of the S/S contact area at electrode failure (at about 65 mm^2) with the initial S/S contact area (at approximately 53–55 mm^2) indicates that about 20% increase of the contact area would result in 20% reduction in current density, and 20% decrease in joint strength (which is correlated to nugget area, as seen in Fig. 5). The existence of the thresholds between the first and second data groups means that the E/S and S/S contact areas increased rapidly around the point of elec-

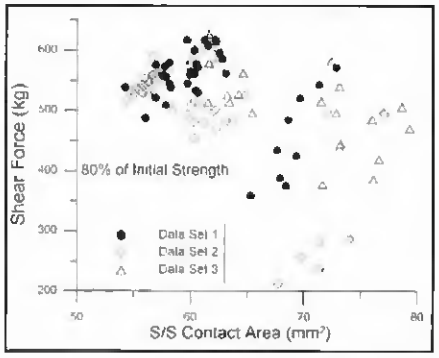

Fig. 10 — Relation between shear force and S/S contact area.

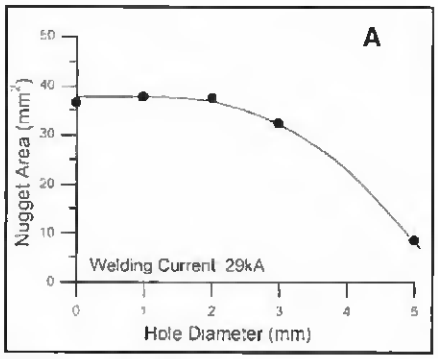

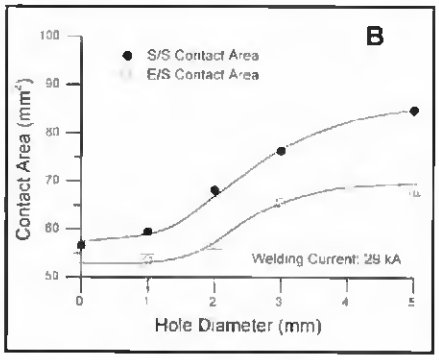

Fig. 11 — Effect of the central hole size on (A) nugget area and (B) contact areas in the simulation test

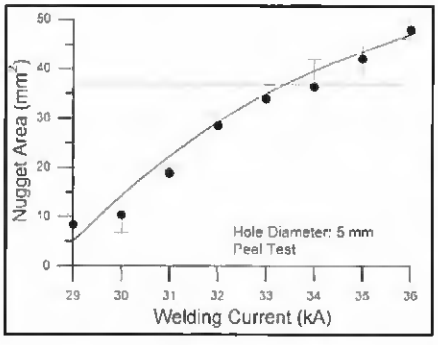

Fig. 12 — Effect of welding current on nugget area in the simulation test.

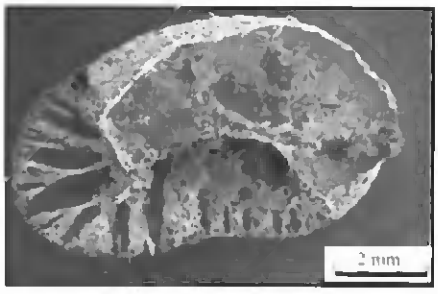

Fig. 13 — Partial button failure due to wormholes at the edge of a nugget.

trode failure. This may also be seen from the changes in the E/S and S/S contact areas just before the electrode failure — Fig. 7. The rapid increase in contact areas appeared to be related to the sudden disappearance of the central portion (i.e., formation of the central, large cavities) of the electrode tip face (at about 360, 810, and 480 welds in Fig. 6). The E/S contact area did not increase significantly while the ring pit grew toward the center. Once the large cavities formed, the E/S contact area would increase by extending the ring contact areas surrounding the cavities to resist the same electrode force (Ref. 10).

It is suggested that the E/S contact area could be used to monitor electrode degradation and predict electrode failure. Although the same trends were found for the tip-face area and the S/S contact area, extra work is needed to monitor these two areas by carbon imprinting and/or destructive testing.

Electrode Pitting

The pitting mechanisms in RSW of aluminum Alloy 5182 have been studied and documented in detail in a separate paper (Ref. 11). The results indicated that electrode degradation, which eventually leads to weld failure, could form in four basic steps: aluminum pickup, electrode alloying with aluminum, electrode tip face pitting, and cavitation. Aluminum pickup began even from the first weld as tiny drops of molten Al were transferred from the sheet surface to the electrode tip face. This molten Al adhered to and reacted with the electrode forming local, complex regions of Cu-Al alloys. The breaking up of the local bonds/alloyed regions, either through transfer of molten Cu-Al mixture or brittle fracture of solidified Cu-Al intermetallic phase(s), would result in electrode pitting, i.e., material loss from the tip face. Initial pitting occurred on a ring near the periphery of the contact area and then grew both inward and outward to form large cavities by combining smaller pitted areas. It is presumed that the pitting process would be very sensitive to the surface conditions (e.g., the oxide thickness). This may be the reason that the electrode life varies considerably even though all the process conditions were nominally kept constant.

To further confirm the correlation between electrode degradation and electrode life, the effects of the electrode central cavity were simulated using electrodes with predrilled central holes on the electrode face. These holes (from 1 to 5 mm in diameter and 2 mm in depth) were drilled before welding. The same welding parameters (Table 2) were used in the simulation. The results (Fig. 11A) indicated that the nugget area started to decrease when the hole diameter was larger than 3 mm and dropped significantly when the diameter was 5 mm. Increasing the hole diameter resulted in an increase in the nominal E/S and hence actual S/S contact areas — Fig. 11B. This increase in the S/S contact area would reduce current density and hence heat generation for nugget formation. Therefore, this simulation has clearly indicated that undersized nuggets are caused by increased contact areas because of degraded electrodes. By increasing welding current for the electrode with 5-mm hole diameter (Fig. 12), the nugget area could be recovered when the current was increased to 34 kA. This further confirms the importance of current density.

Weld Defects

In this work, joint strength, determined by shear testing, was correlated to nugget area. However, button diameter, measured from the button left at the faying surface in peel testing, is sometimes used to determine joint quality. In this case, the button diameter, which may not necessarily equal the nugget diameter, could be affected by many factors (such as weld expulsion and porosity distribution) other than current density. Figure 13 shows a partial button pullout produced by peel testing, in which the button size was found to be smaller than the nugget area. Wormholes appeared to be the reason for the partial button pullout in this case. It has been reported that these defects, especially when formed at the edge of a nugget, affect the joint quality, and hence, electrode tip life (Ref. 15). Moreover, Gean et al. (Ref. 16) reported that porosity increased with reduction of electrode force. It is believed that the formation of pores at the edge of a nugget is caused by inhomogeneous current and pressure distribution. However, further work is needed to investigate the details of how such factors affect the failure modes of button pullout in peel tests.

Summary

Electrode life tests were conducted to investigate the effects of electrode degra-

dation on electrode life, in resistance spot welding of 1.5-mm-thick sheet aluminum Alloy 5182 using a medium-frequency direct-current welding machine and electrodes with a tip face curvature radius of 50 mm and tip face diameter of 10 mm.

The observed electrode life in several electrode life tests ranged from about 400 to 900 welds even though all the process conditions were intentionally kept constant. However, despite the large variation, distinct patterns were found to correlate electrode failure to electrode degradation in terms of the change in tip-face and contact areas at both E/S and S/S interfaces:

- Stage 1: At the beginning of the electrode life, the tip-face area and joint strength were relatively constant.
- Stage 2: In this period, the joint strength increased and peaked. Incipient electrode pitting was observed right before the strength peaked. The nominal tip-face area, and hence the contact areas at both E/S and S/S interfaces, started to increase after the onset of electrode pitting.
- Stage 3: The joint strength started to drop, as the tip-face and contact areas continued to increase because pitted areas grew and combined into large cavities, until the electrode failed.

The reduction in joint strength was caused by undersized nugget formation due to increased contact areas and hence reduced current density. The electrode degradation may be monitored by the increase in all three areas (tip-face area, and E/S and S/S contact areas), but the E/S contact area is believed to be the most suitable because the least extra work is needed to measure it. The button diameter, measured from peel testing, may not necessarily equal the nugget diameter and could be affected by many factors (such as weld expulsion and porosity distribution) other than current density.

Acknowledgments

This study has been supported by the Natural Sciences and Engineering Research Council (NSERC), and the Automobile of the 21st Century (AUTO21), one of the Networks of Centres of Excellence (NCE) programs, both established by the Canadian government. Experimental assistance from Mr. X. Li and J. Mui from the University of Waterloo in this study is greatly appreciated.

References

1. Irving, B.1995. Building tomorrow's automobiles. *Welding Journal* 74(8): 29–34.

2. Williams, N. T. 1984. Suggested topics for future research in resistance welding. *Welding in the World* 22(1/2): 28–34.

3. Matsumoto, J., and Mochizuki, H. 1994. Spot welding of aluminium alloy — Electrode life for various electrodes. *Welding International* 8(6): 438–444.

4. Rivett, R. M., and Westgate, S. A. 1980. Resistance welding of aluminium alloys in mass production. *Metal Construction* 12(10): 510–517.

5. Glagola, M. A., and Roest, C. A. 1976. Nickel plated electrodes for spot welding aluminum. SAE paper 760167.

6. Ikeda, R., Yasuda, K. Hashiguchi, K., Okita, T., and Yahaba, T. 1995. Effect of electrode configuration on electrode life in resistance spot welding of galvannealed steel and aluminum alloy for car body sheets. *Proc. Advanced Technologies & Processes (IBEC '95)*, pp. 44–51.

7. Leone, G. L., and Altshuller, B. 1984. Improvement on the resistance spot weldability of aluminum body sheet. SAE paper 840292.

8. Rivett, R. M. 1980. Spot welding electrode life tests on aluminium sheet — Effect of parent metal composition and surface treatment. *The Welding Institute* 132/1980.

9. Patrick, E. P., and Spinella, D. J. 1996. The effects of surface characteristics on the resistance spot weldability of aluminum sheet. *AWS Sheet Metal Welding Conference*, Paper No. B4, Troy, Mich.: AWS Detroit Section 7.

10. Lum, I. 2002. Electrode deterioration in the medium frequency DC resistance spot welding of 5182 aluminum alloy. M.A. Sc. thesis, University of Waterloo.

11. Lum, I., Fukumoto, S., Biro, E., Boomer, D. R., and Zhou, Y. 2003. Electrode pitting in resistance spot welding of aluminum alloy 5182. Accepted for publication, *Metall. Mater. Trans. A.*

12. Thornton, P. H., Krause, A. R., and Davies, R. G. 1996. The aluminum spot weld. *Welding Journal* 75(3): 101-s to 108-s.

13. Van Horn, K. R. 1967. *Aluminum*, Vol. 1, Materials Park, Ohio: ASM International, pp. 303–336.

14. Hasir, M. 1984. A study of the Peltier effect in the resistance spot welding of very thin-gage sheet electroplated with tin using tungsten insert electrodes. *Welding and Cutting* 36(3): 116–121.

15. Chuko, W., and Gould, J. 2000. Metallurgical interpretation of electrode life behavior in resistance spot welding of aluminum sheet. *Proc. Joining of Advanced and Specialty Materials*, pp. 114–121. St. Louis, Mo.: ASM International.

16. Gean, A., Westgate, S. A., Kucza, J. C., and Ehrstrom, J. C. 1999. Static and fatigue behavior of spot-welded 5182-O aluminum alloy sheet. *Welding Journal* 78(3): 80-s to 86-s.

2004 Poster Session
Call for Entries

The American Welding Society announces a Call for Entries for the 2004 Poster Session to be held as part of Welding Show 2004 on April 6–8, 2004, in Chicago, Ill. Students, educators, researchers, engineers, technical committees, consultants, and anyone else in a welding- or joining-related field are invited to participate in the world's leading annual welding event by visually displaying their technical accomplishments in a brief graphic presentation, suitable for close, first-hand examination by interested individuals.

Posters provide an ideal format to present results that are best communicated visually, more suited for display than verbal presentation before a large audience; new techniques or procedures that are best discussed in detail individually with interested viewers; brief reports on work in progress; and results that call for the close study of photomicrographs or other illustrative materials.

Submissions should fall into one of the following two categories and will be accepted only in a specific format. Individuals interested in participating should contact Dorcas Troche, Manager, Conferences & Seminars, via e-mail at *dorcas@aws.org* for specific details. Deadline for submission of entries is Monday, December 1, 2003.

1. Student Division
   - Category A: 2-Year or Certificate Program
   - Category B: Undergraduate Degree
   - Category C: Graduate Degree

2. Professional/Commercial Division